JOURNAL OF MATERIALS SCIENCE 22 (1987) 4313–4325

Surface treatment of sillimanite-based microspheres for strength enhancement of high-temperature lightweight cement composites

T. SUGAMA, L. E. KUKACKA, B. G. GALEN, K. WOO
Process Sciences Division, Department of Applied Science, Brookhaven National Laboratory, Upton, New York 11973 USA

The compressive strength of high-temperature lightweight cementing materials containing sillimanite-based hollow microspheres as a filler can be improved by treating the surfaces of the microspheres with a calcium hydroxide-saturated solution at temperatures up to 200° C. The precipitation of an epitaxial layer formed by an interaction between the hot calcium hydroxide solution and the surface of the sphere played an essential role in developing favourable bonding characteristics at the interfaces and in promoting the hydration of the cement matrix. Bonding is associated with the formation of an intermediate layer of aluminium-rich calcium silicate hydrate, produced by an interfacial reaction of the cement paste with the epitaxy, under the hydrothermal environment at 300° C. A dense intermediate layer consisting of a rim structure of 4 μm thickness acts in cross-linking and coupling functions that serve to connect the cement matrix and spheres, thereby improving the interfacial bond strength. The presence of the epitaxial layer on the treated sphere surfaces leads to the formation of a well-crystallized tobermorite matrix phase, which is responsible for the development of strength in autoclaved lightweight cements.

1. Introduction

The use of normal-density 1.7 to 1.9 g cc^{-1} cementing slurries in completing geothermal wells frequently results in problems of lost circulation when attempts are made to cement the well in regions that pass through weak unconsolidated rock zones having very fragile gradients. Specifically, these unconsolidated formations fracture as a result of the high hydrostatic pressures required to pump the highly dense cement slurries. To avoid this problem, high-temperature low-density cement slurries are needed to support the intermediate casing pipe and to protect the casing from corrosive fluids and gases.

There are two methods for the preparation of lightweight cement slurries which can be used in geothermal wells. One method is to introduce air bubbles into an ordinary cement slurry that has an adequate cement-to-silica ratio [1]. The resulting small, fine foam bubbles which are dispersed uniformly within the slurries are thought to promote stronger cement walls around the bubbles and so provide a set cement of increased integrity. Discrete bubble formation produced by incorporating a graphite fibre also is important in creating high-quality foam cement slurries. In this case, discrete bubbles under high pressure conditions are chemically and physically stabilized as microscopic cells within the cement slurry until the cement sets; this produces a hardened foam cement with adequate compressive strength and low permeability to water and gas.

A second method is to incorporate pressure-resistant hollow microspheres into cement slurries [2]. In addition to producing a lightweight slurry, the relatively high bridging ability of the hollow beads enhances its effectiveness in controlling lost-circulation problems. However, results from our preliminary studies on the preparation of microsphere-filled lightweight cement systems suggested that the inclusion of the microspheres as a filler was not sufficient to yield the properties needed for geothermal cements. For instance, when a slurry with a density of 1.16 g cc^{-1} was autoclaved for 24 h at a temperature of 300° C and a hydrostatic pressure of 10.3 MPa, the compressive strength of the set cement paste was only 4.2 MPa. The low strength was presumed to be due to poor bonding at the cement-microsphere interface, and a low degree of hydration in the cement matrixes and the interfacial regions. Therefore, modification of the microsphere surfaces was deemed necessary to produce a high-quality high temperature light-weight cementing material that could meet the criteria. These changes included a slurry density of < 1.2 g cc^{-1} at 25° C, a 300° C–24 h compressive strength of > 6.9 MPa, and a bulk density of < 1.0 g cc^{-1}.

With regard to adhesion at cement-glass or silica aggregate interfaces, several investigators suggested that the epitaxial growth of certain hydration products (such as ettringite, calcium hydroxide, and calcium silicate hydrate) precipitated on the aggregate surfaces is mainly responsible for the development of

0022–2461/87 $03.00 + .12

the cement-aggregate bonds [3–5]. The mode of interfacial contact zone was schematically proposed by Zimbelmann [6]. He suggested that the contact zone consists of a contact layer, formed as an inductive deposition step at the outermost surface-sites of the aggregate, and an intermediate layer superimposed on the surface of the contact layer. The main constituents of the contact layer, which has a thickness of 2 to 3 μm, were ettringite which is enveloped by calcium hydroxide crystals lying perpendicular to the aggregate surface. Complexes of calcium hydroxide and calcium silicate hydrate settle in an $\sim 20\,\mu$m thick intermediate layer. Without an exceedingly rough aggregate surface morphology, any improvement in the interfacial bond strength seems to depend upon the species of the precipitated cement hydration products, which may contribute to the mechanical and chemical coupling functions connecting the hardened cement matrix with the aggregate. Regardless of the coupling mechanism, which may be a mechanical interlocking or a chemical reaction, the epitaxially growth calcium hydroxide and calcium silicate hydrate crystals seem to play an essential role in promoting good interfacial bonds at the cement-aggregate joints.

Based upon the literature, we anticipated that if the surface of the spherical-shaped filler was covered with a reactive calcium-based hydrate layer, the addition of the modified spheres to a cement paste would give a higher strength lightweight cementing material. Thus, the surfaces of spheres were treated with a saturated solution of calcium hydroxide at temperatures up to 300° C to determine if a highly reactive surface could be produced. Our major objective was to understand how the chemical states and phase morphologies of hydrate products formed on sphere surfaces modified by hot alkali solutions improve the compressive strength of sphere-filled cement specimens after autoclaving at 300° C. The first approach focused on the identification of chemical and morphological transformations occurring on the surface of the treated spheres. The consequential data led to the formulation of a possible reaction mechanism between calcium hydroxide and sphere surfaces in hydrothermal environments. Then, to explore the coupling and cross-linking mechanisms of interfacially formed hydration products, emphasis was given to an investigation of the chemical elements and micromorphological structure at the contact zones near the sphere particles. This was correlated indirectly with the phase relations and the degree of hydration in the matrix of the bulk cement paste.

2. Experimental procedure

2.1. Materials

The lightweight filler used was pressure-resistant hollow microspheres, having an average particle size of $\sim 125\,\mu$m and a bulk density of $0.4\,\mathrm{g\,cc^{-1}}$, supplied by Fillite U.S.A., Inc. An API class H cement, supplied by the Lehigh Portland Cement Co., was used as the matrix. A typical analysis of the cement was: 64.4 wt % CaO, 22.4 wt % SiO_2, 4.29 wt % Al_2O_3, 4.92 wt % Fe_2O_3, 0.8 wt % MgO, and 2.2 wt % SO_3. To prevent retrogression of strength at high temperatures, silica flour having a particle size of $< 44\,\mu$m was added to the cement.

The surface modification of the microspheres was accomplished as follows. The microsphere surfaces first were rinsed with deionized (D.I.) water to remove any contamination and then exposed for ~ 20 h in a saturated solution of calcium hydroxide at a temperature of up to 300° C. Then the microspheres were again washed in D.I. water and subsequently dried in an oven at 110° C. Microspheres treated with only the D.I. water at temperatures up to 300° C were employed as controls.

Microsphere-filled lightweight cements, used to determine compressive strength and to explore cement-microsphere interfaces, were prepared the following way. The lightweight cement slurries, consisting of 30 wt % class H cement, 10 wt % silica flour, 25 wt % microspheres, and 35 wt % water were poured into glass test tubes, 3.5 cm diameter by 7.0 cm long. The test tubes then were autoclaved for 24 h at 300° C.

2.2. Measurements

The chemical states and elemental compositions at the surface sites of treated and untreated microspheres were identified by precise determinations of bonding energies and peak intensities with X-ray photoelectron spectroscopy (XPS). The spectrometer used was a V.G. Scientific ESCA 3 MK II; the exciting radiation was provided by a Mg $K\alpha$ X-ray source, operated at a constant power of 200 W (10 kV, 20 mA). The vacuum in the analyzer chamber of the instrument was maintained at 10^{-9} Torr.

The morphological and chemical aspects of the surface and subsurface of treated microspheres, and the cement hydration products formed in the cement-sphere contact zone were examined with an AMR 10 nm scanning electron microscope (SEM) associated with TN-2000 energy-dispersive X-ray spectrometry (EDX).

X-ray powder diffraction analyses (XRD) were used to identify the phases present in the hydrated cement matrix and to determine the chemical constituents of the shell materials in the hollow microspheres.

3. Results and discussion

3.1. Surface characteristics of modified and unmodified spheres

Fig. 1 shows a typical micrograph of the unmodified "as-received" hollow microspheres. The microspheres range in size from ~ 30 to $\sim 200\,\mu$m, and it was estimated from profiles of fragments from fractured spheres that the wall thickness is $\sim 10\,\mu$m.

The chemical constituents of the shell material responsible for the high shear strength and high pressure resistance of the microspheres were identified by XRD analysis in the diffraction range from 0.553 to 0.206 nm (Fig. 2). The XRD pattern shows the presence of two major silicon compounds. One is sillimanite, $Al(AlSiO_5)$ [7], which is characterized by two prominent lines at 0.337 and 0.22 nm, medium intensities at 0.341, 0.269, and 0.253 nm, and relatively weak diffractions at 0.535, 0.288, 0.242, 0.229, and 0.221 nm. The remaining strong line at 0.334 nm

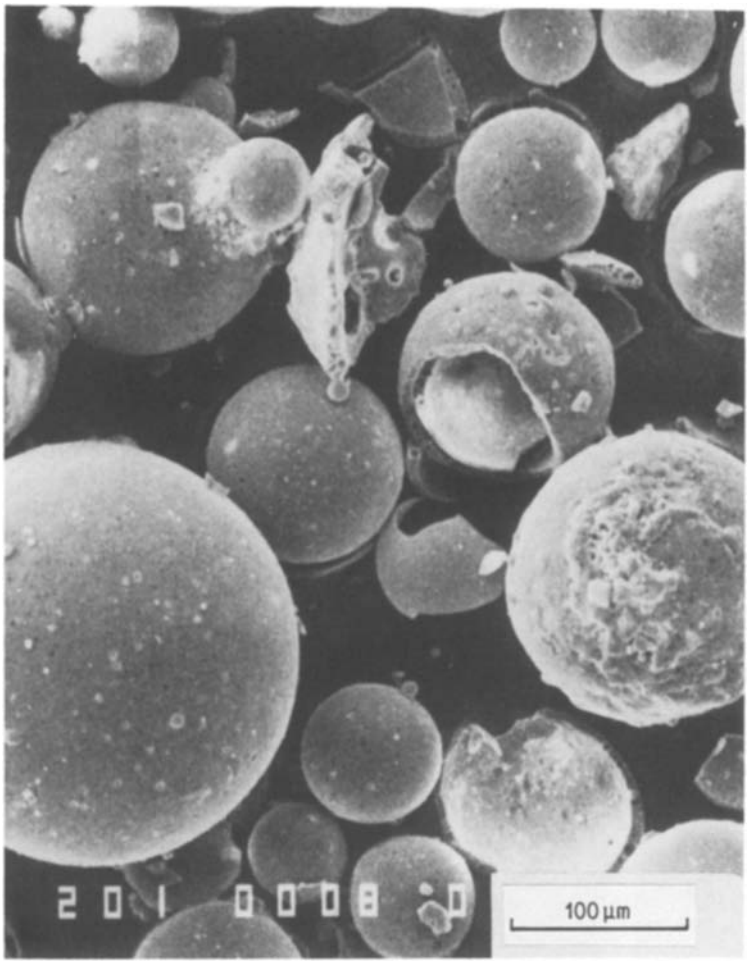

Figure 1 Scanning electron micrograph of unmodified microsphere filler.

indicates the presence of quartz as the second major component. Thus, the shell structure of the hollow microspheres appears to be an assemblage of hybrid phases of sillimanite and silica glass.

Figs 3 and 4 show scanning electron microscopy (SEM) micrographs with accompanying energy-dispersive X-ray spectrometer (EDX) analyses, and X-ray photoelectron spectroscopy (XPS) wide survey scans, respectively. Results are given for untreated sphere surfaces, spheres treated with D.I. water at 200° C, and spheres treated with a saturated solution of calcium hydroxide at 100° C. EDX is extremely useful for the quantitative analysis of any elements which exist on a surface solid layer up to $\sim 2\,\mu m$ in thickness. The abscissa of the EDX spectrum is the X-ray energy characteristic of the element, and the intensity of a gross peak count relates directly to the amount of each element present.

In contrast, XPS can be used to identify the chemical states and to obtain quantitative elemental analyses for thin surface films ranging from 0.5 to 5 nm. Identification can be made from precise determinations of binding energies (BE), peak shapes, and other spectral features. Quantitative assessments are made from comparisons between XPS peak heights. Therefore, EDX techniques for subsurface analyses and

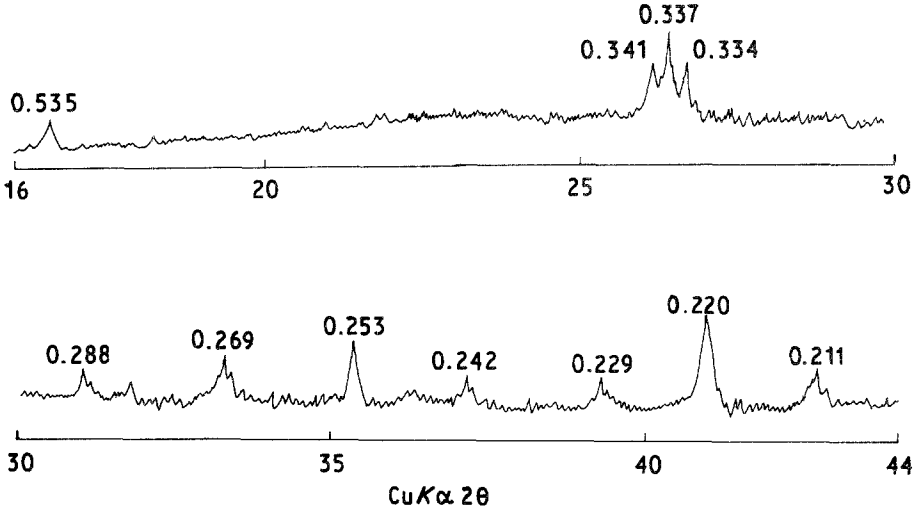

Figure 2 XRD pattern of shell material in "as-received" hollow microspheres. Values are in nm.

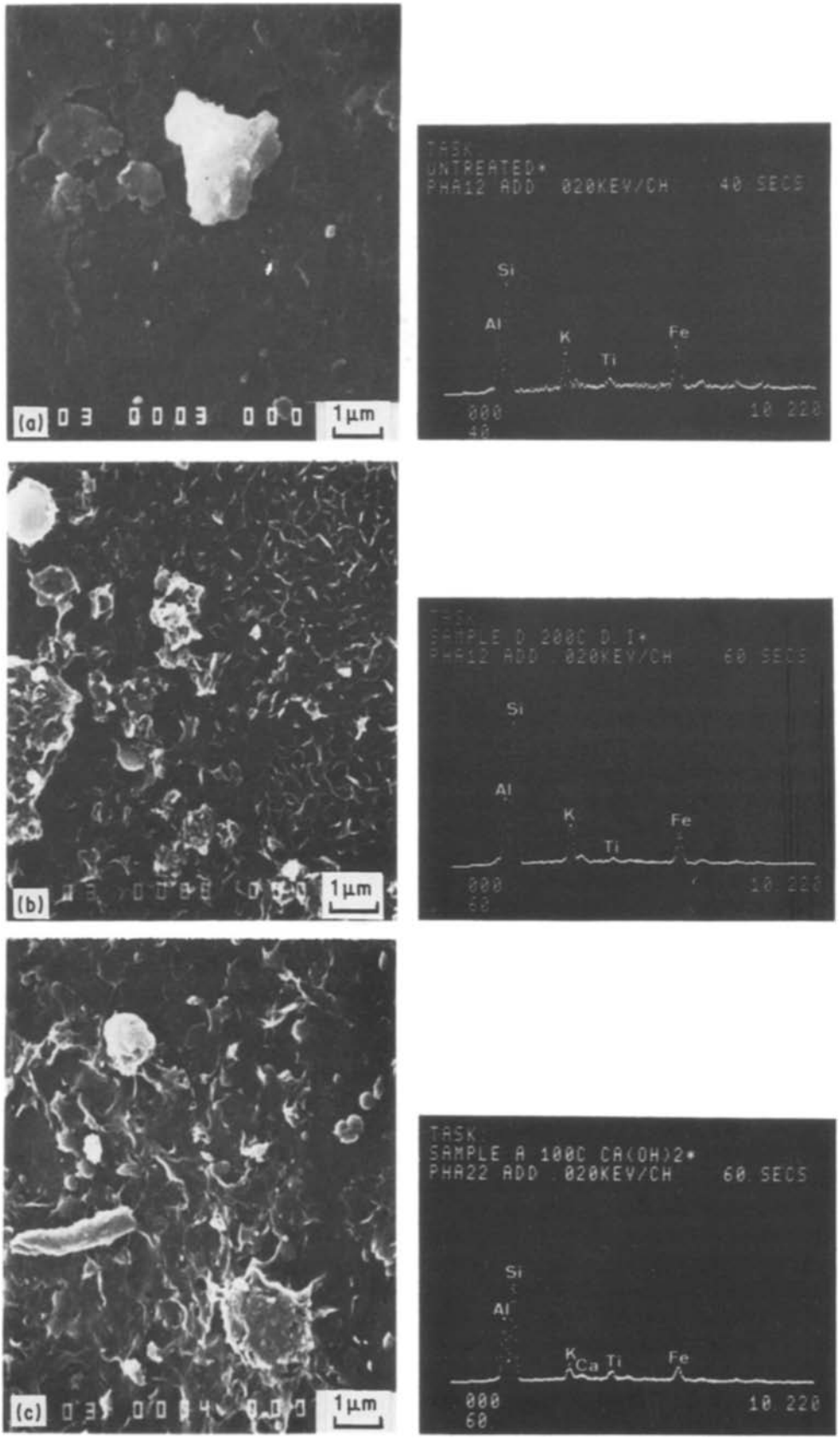

Figure 3 Surface morphological and EDX elemental data for (a) untreated, (b) 200°C D.I.-treated, and (c) 100°C $Ca(OH)_2$-treated microspheres.

XPS for the surface can greatly enhance the results and facilitate the interpretation of SEM surface studies.

The surface morphology of the untreated spheres is relatively smooth suggesting that they are mostly free of irregularities or deposits (Fig. 3a). The EDX spectrum for this sample indicates that the predominant element present is silicon, with lesser amounts of aluminium, potassium, and iron. The weak peak shows that a small quantity of titanium is also present.

The XPS spectrum for the unmodified sphere surfaces shows the presence of an intense O_{1s} peak and a secondary strong carbon (C_{1s}) peak (Fig. 4). The latter

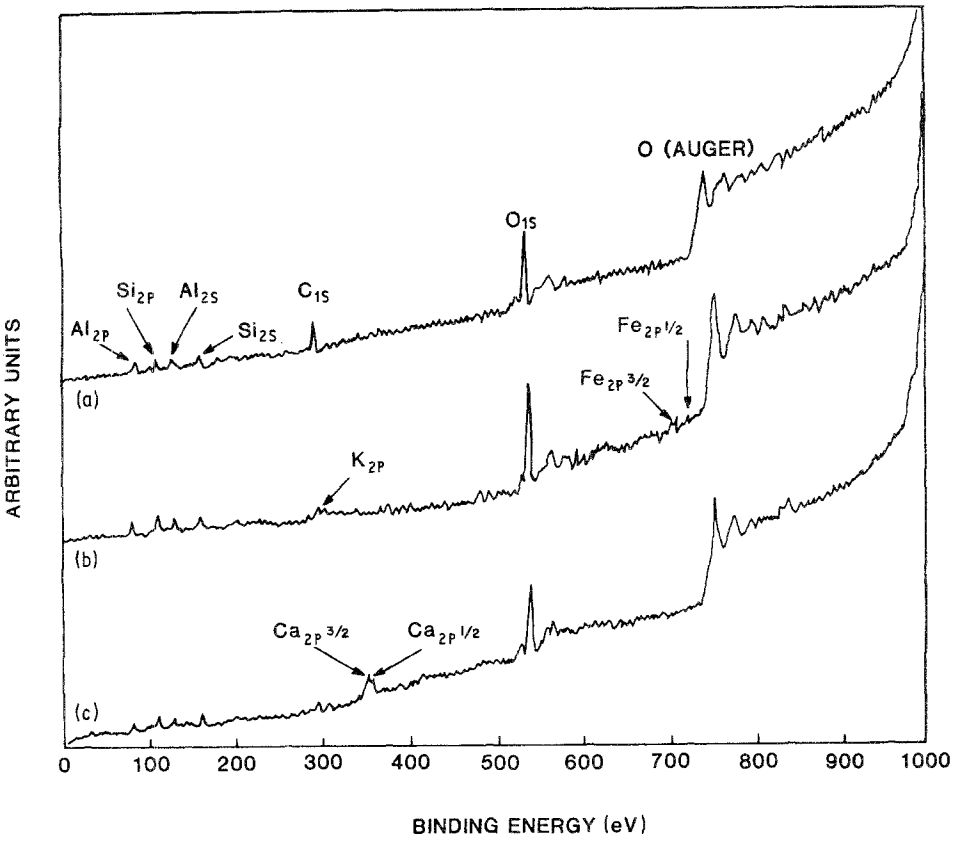

Figure 4 XPS survey-scan spectra for untreated (a), 200° C D.I.-treated (b) and 100° C calcium hydroxide-treated spheres (c).

is mainly ascribed to the residual carbon contaminants. Small aluminium (Al_{2p} and Al_{2s}) and silicon (Si_{2p} and Si_{2s}) signals also were identified. However, the signal intensities of potassium, titanium and iron which were clear on the EDX analysis are too weak to be detected on the wide scan at the maximum count rate of 10800 C.P.S. Thus, the unmodified sphere surfaces appear to be overlaid with a thin film consisting of oxidized aluminium, silica glass, and a carbon contaminant. All of the potassium, titanium and iron seem to exist at the subsurfaces. Such thin surface films are removable.

Comparing micrographs in Figs 3a and b, it is apparent that the originally smooth surface of the "as-received" spheres was transformed into a geometrically reticulated network by exposure to D.I. water at 200° C. This morphological transformation reveals the characteristics of the underlying structure and indicates that the thin overlay can be removed by hot D.I. water. It should be noted that D.I. treatment at 100° C is too low to remove the film, suggesting that the glass and carbon adhere tightly to the underlying materials. The typical network structure of lath-like crystals in the underlying material beneath the thin film must be associated with the formation of sillimanite, $Al(AlSiO_5)$, as the major phase of the shell structure. Referring to the EDX data in Fig. 3b, the conspicuous growth of the silicon peak suggests that the underlying crystalline materials contain a large amount of silicon compounds. No significant changes in peak intensity were observed for elements such as aluminium, potassium, titanium and iron.

Fig. 4 shows an XPS wide scan for the 200° C D.I.-treated sphere surface. Compared with the untreated surface, the scan is characterized by intense aluminium, silicon and oxygen signals, the appearance of identical potassium and iron peaks, and a considerable reduction in carbon peak intensity. The probable reason for the latter is the elimination of carbon contamination by the hot D.I. water treatment. Detailed information and its elucidation regarding the increased aluminium and silicon peak intensities and the newly grown potassium and iron signals is discussed subsequently under "High-Resolution Spectral Studies".

Of particular interest are the morphological transformations which occur on the sphere surfaces modified by the calcium hydroxide-saturated solution at 100° C (Fig. 3c). The SEM image exhibits a morphologically peculiar surface that consists of a layer of elongated crystals, providing evidence of epitaxial growth of certain hydration products. The epitaxy is topographically identical to the formation of a continuous layer overlaid on the sphere surface. The continuous epitaxy film seems to form a shell structure that encapsulates the sphere particle. The EDX spectrum for this hydration shell reveals noteworthy reductions in the intensities of the silicon, potassium, titanium and iron peaks, confirming the calcium signal and an unchanged aluminium peak (Fig. 3c). The presence of the calcium peak relates directly to the reaction products at the interface between the calcium hydroxide and the chemical composites of the sphere surface, and the calcium hydroxide precipitated on the sphere. The reduction in the peaks for silicon, potassium, titanium and iron elements may indicate that the sphere was covered by calcium hydration products to a depth of at least 1 μm. The essentially constant aluminium intensity for both the calcium hydroxide- and the D.I.-treated spheres verifies that a relatively large amount of aluminium is present in the epitaxy layers.

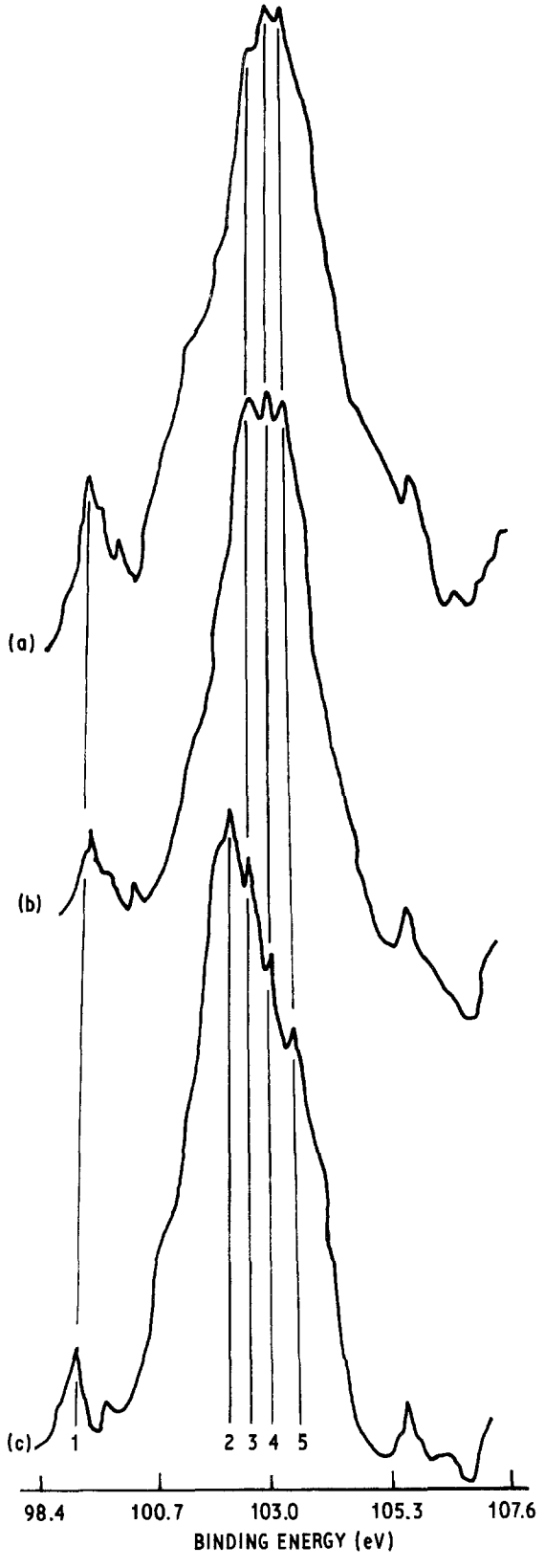

Figure 5 Si_{2p} core level spectra from the surface of (a) untreated, (b) 200° C D.I.-treated and (c) 100° C calcium hydroxide-treated microspheres. Peak assignments are: (1) silicon at 99.6 eV, (2) $CaO-SiO_2-H_2O$ or $CaO-Al_2O_3-SiO_2-H_2O$ systems at 102.2 eV, (3) sillimanite at 102.6 eV, (4) cristobalite at 103.1 eV, (5) quartz at 103.5 eV.

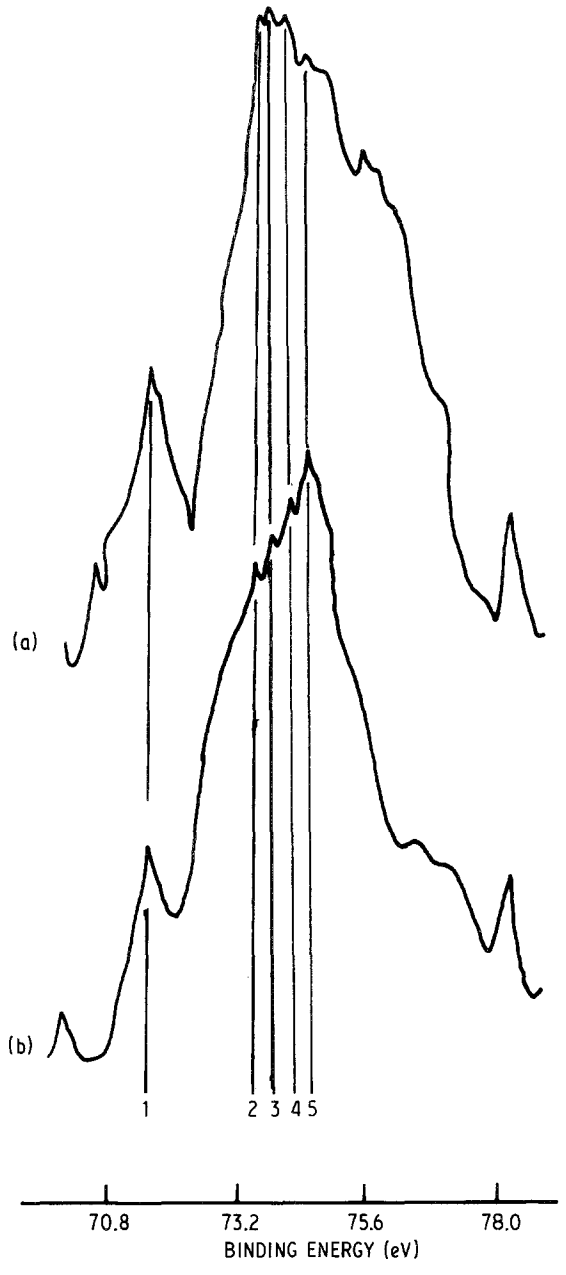

Figure 6 Al_{2p} spectra from the surface of (a) untreated and (b) 200° C D.I.-treated spheres: (1) Aluminium at 72.1 eV, (2) γ-Al_2O_3 at 73.6 eV, (3) α-Al_2O_3 at 73.9 eV, (4) bayerite or boehmite at 74.3 eV, (5) sillimanite at 74.6 eV.

Generally, direct phase data for the outermost surface sites of spheres are very difficult to obtain using X-ray diffraction analysis because of the limited amount of material available. However, XPS high-resolution spectrum analysis is very useful for precise phase identifications.

Let us consider in detail the XPS data from untreated and treated sphere surfaces. Figs 5 and 6 show high-resolution spectra for the Si_{2p} and Al_{2p} core levels for the untreated, 200° C D.I.-treated, and 100° C calcium hydroxide-treated sphere surfaces. The BE of the spectrum can be used to manifestly identify the presence of a particular group. The possible chemical transformations and the specific groups existing on the sphere surfaces were determined by means of the peak fitting procedure in differentiating between the surface chemical compositions. The arbitrarily chosen BE widths ranged from 98.4 to 107.6 eV for the Si_{2p} signal, and 70.8 to 78.0 eV for the Al_{2p}. The original Si_{2p} spectrum for the untreated surface in Fig. 5a involves four major peaks: 99.6, 102.6, 103.1, and 103.5 eV. The two highest intensity peaks at 103.1 and 103.5 eV (identified as No. 4 and No. 5, respectively) can be ascribed to be the presence of cristobalite and quartz, respectively. The secondary strong peak at 102.6 eV (No. 3) reveals the formation of sillimanite.

The weak peak of No. 1 at 99.6 eV is associated with the presence of silicon.

The broad Al_{2p} spectrum for the untreated surface is given in Fig. 6a. As evident from the principal line position, the data strongly indicate the presence of three major aluminium species; γ-Al_2O_3 at 73.6 eV (No. 2), α-Al_2O_3 at 73.9 eV (No. 3), and bayerite, $Al(OH)_3$ or boehmite, AlO(OH) at 74.3 eV (No. 4), at the outermost surface sites of the sphere.

A result similar to that for the Si_{2p} spectrum was obtained from the extent of signal growth of sillimanite at 74.6 eV, namely, its peak intensity was confirmed as a secondary line position. The lowest assignment at 72.1 eV corresponds to the presence of aluminium. Therefore, the removable thin continuous overlayer formed on the underlying shell material appears to be composed primarily of a carbon contaminant, cristobalite, quartz, γ- and α-Al_2O_3, and hydrated aluminium oxides, such as bayerite or boehmite. Sillimanite seems to be formed beneath the hybrid overlay surfaces, as verified from analyses of the Si_{2p} and Al_{2p} spectra for 200° C D.I.-treated spheres (Figs 5b and 6b). The sillimanite peaks for Si_{2p} (No. 3) and for Al_{2p} (No. 5) exhibited noteworthy growth in the highest-intensity position. In contrast, the peak intensities of oxidized and hydrated aluminium species were reduced significantly. This information, and the morphological transformations observed made in the SEM study strongly suggest that some parts of the overlays were removed by the hot D.I., so that the sillimanite phase appears as the underlying material.

After eliminating the aluminium- and silicon dioxide-based overlayers and the carbon contaminant, the surface of the freshly disclosed underlying material is composed of sillimanite and of some iron- and potassium-based compounds, as recognized in the XPS wide scan survey (Fig. 4). To identify the iron-rich compounds which were mixed with the sillimanite, a high-resolution examination of $Fe_{2p3/2}$ was accomplished over a BE range of 706.5 to 714.0 eV. The results yielded several unidentified peaks, but at least three different iron species are present as the major Fe compounds (Fig. 7). The peak at 711.7 eV is due to the contribution of the magnetite, Fe_3O_4. The strongest peak at 711.0 eV might be ascribed to the substantial concentration of maghemite, γ-Fe_2O_3, and the control iron peak at 710.5 eV may reveal the presence of wuestite, FeO. The spectrum for the $K_{2p3/2}$ core level exhibited too much noise to be analyzed. This suggests that the quantity of potassium compounds on the underlying material surfaces is very small.

On the basis of information from the XPS and SEM-EDX techniques, the underlying crystalline materials which are representative of the reticulated network structure of lath-shaped particles, appear to be composed of mixed multiple phases of sillimanite as a major product, and oxidized and hydrated compounds of silicon, aluminium and iron as a minor phase. It was inferred that the spaces between the lath-like crystals may be occupied by such elements as silicon, aluminium and iron. This formation appears to be responsible for the resulting high pressure-resistant spherical shell structure.

Figure 7 $Fe_{2p3/2}$ spectrum of 200° C D.I.-treated sphere surface: wuestite at 710.5 eV, maghemite at 711.0 eV and magnetite at 711.7 eV.

Let us return to the Si_{2p} spectra in Fig. 5. Considerable attention was given to the different shape of the spectrum for the 100° C calcium hydroxide-modified sphere surfaces, as depicted in Fig. 5c. The spectrum was characterized by a new and predominant peak at 102.2 eV (No. 2) and three additional shoulder peaks. The pronounced line assignment at 102.2 eV is believed to be due to the presence of calcium silicate hydrate ($CaO-SiO_2-H_2O$) or calcium aluminate silicate hydrate ($CaO-Al_2O_3-H_2O$) systems which can be explained as the most abundant chemical states at the outermost surface sites of the treated spheres. As explicated from the shoulder peak at 102.6 eV, the sillimanite seems to exist underneath the $CaO-SiO_2-H_2O$ or $CaO-Al_2O_3-SiO_2-H_2O$ system layers. The conspicuous reduction in line intensities for the silicon dioxide species at 103.1 and 103.5 eV peaks indicates that the silicon dioxide, which was identified as one of the major constituents on untreated sphere surfaces reacted chemically with the hot calcium hydroxide solution to precipitate the $CaO-SiO_2-H_2O$ system. This interfacial chemical reaction apparently leads to the morphological transformation into the continuous $CaO-SiO_2-H_2O$ or $CaO-Al_2O_3-SiO_2-H_2O$ layers deposited directly onto the sphere surface.

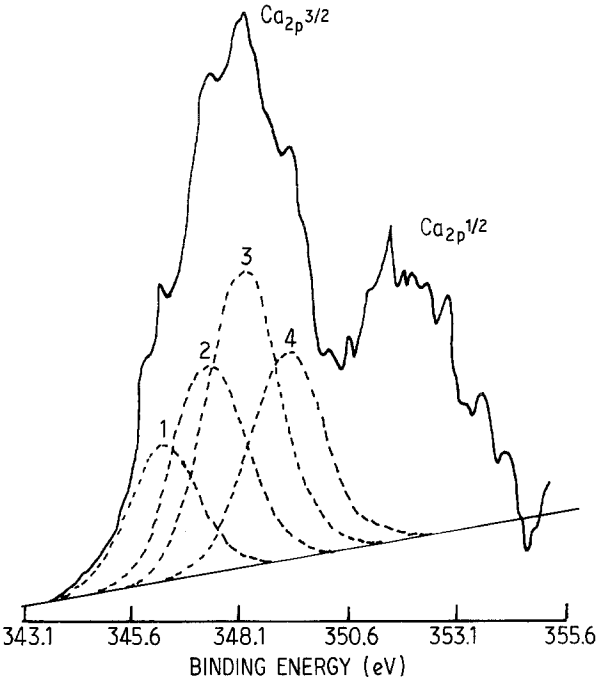

Figure 8 $Ca_{2p3/2}$ and $_{2p1/2}$ spectra of 100° C calcium hydroxide-treated sphere surface: (1) Calcium hydroxide at 346.7 eV, (2) $CaO-SiO_2-H_2O$ system at 347.6 eV, (3) $CaO-Al_2O_3-SiO_2-H_2O$ system at 348.4 eV, (4) unknown at 349.1 eV.

The XPS study was extended to obtain detailed information regarding the calcium-based hydrates formed on the calcium hydroxide-treated sphere surfaces. The consequent spectrum for the $Ca_{2p3/2}$ core level in the BE range of 343.1 to 350.6 eV is illustrated in Fig. 8. This spectrum was reconstructed from the four major peaks which represent the presence of four distinct calcium species. The lowest BE at 346.7 eV is due to unreacted and residual calcium hydroxide. The calcium in $CaO-SiO_2-H_2O$ is readily identifiable from the secondary low BE level (No. 2) at 347.6 eV. The principal line arising at 348.4 eV (No. 3) is possibly associated with the presence of the calcium aluminate silicate hydrate ($CaO-Al_2O_3-SiO_2-H_2O$) system. However, the phase present at the 349.1 eV peak is unknown. Nevertheless, the main conversion product precipitated by the chemical interaction between the calcium ions from the calcium hydroxide and the sphere surfaces under the hydrothermal environment is likely to be associated with the formation of the $CaO-Al_2O_3-SiO_2-H_2O$ system, rather than the $CaO-SiO_2-H_2O$ system.

From our observations we can reasonably draw the following empirical evidence for the interaction at the interface between the sphere surface and the calcium hydroxide solution, and for the formation of its reaction products at the interface. When the sillimanite-based microspheres are exposed to the alkaline calcium hydroxide-saturated solution at 100° C, more silicate and aluminate is dissolved from the sphere surface as an essential first step in the chemical reaction. This dissolution significantly promotes the precipitation of epitaxial $CaO-SiO_2-H_2O$ and $CaO-Al_2O_3-SiO_2-H_2O$ formations, produced by the chemical reactions between the dissociated silicon and aluminium with the abundant calcium ions released from the calcium hydroxide solution. With increased hyration, the precipitated layer is overlapped by these epitaxial hydration products. While the epitaxies grow in the vicinity of the sphere surface, the unreactive calcium hydroxide also precipitates in the contact layer formed at the interfacial regions between the spheres and the reaction products. However, the deposited calcium hydroxide seems to be masked entirely within the hydrated reaction product layers. Finally, the continuous contact layer forms a spherical shell structure to fully encapsulate the sphere.

3.2. Formations at cement-sphere interface and phase of hydrated cement matrix

To evaluate the ability of treated sphere surfaces to enhance the compressive strength of sphere-filled lightweight cement systems, cement slurries were prepared consisting of 30 wt % class H cement, 10 wt % silica flour, 25 wt % microspheres, and 35 wt % water. The slurry density for all specimens in this series ranged from 1.16 to 1.20 g cc^{-1}. These lightweight slurries then were autoclaved for 24 h at 300° C.

Table I summarizes the slurry density measurements, and the densities and compressive strengths of the cured specimens. Each value represents the average of three measurements. As expected, the control specimens had a low compressive strength (4.2 MPa). This was greatly improved by treatment of the spheres with either D.I. water or calcium hydroxide. The strength of the specimens made with D.I.-treated spheres appears to depend on the temperature of the treatment. For example, the strength developed in the 100° C D.I.-treated specimens was considerably lower than those at 200 and 300° C. This reduced level of improvement might be associated with the presence of a carbon contaminant on the sphere surface, suggesting that such a contaminant cannot be removed by

TABLE I Properties of microsphere-filled lightweight cementing materials

Treatment of microspheres	Slurry density (g cc^{-1})	300° C-24 h autoclaved specimen	
		Density of set cement (g cc^{-1})	Compressive strength (MPa)
Untreated	1.16	0.90	4.20
100° C D.I.-treated	1.16	0.90	4.44
200° C D.I.-treated	1.17	0.91	7.44
300° C D.I.-treated	1.19	0.92	7.79
100° C calcium hydroxide-treated	1.17	0.91	9.92
200° C calcium hydroxide-treated	1.19	0.91	9.51
300° C calcium hydroxide-treated	1.20	0.95	8.68

D.I. water at 100° C. The strengths for the calcium hydroxide sphere-filled specimens appear to be less dependent on the temperature of the treatment. Here, a maximum strength of 992 MPa was obtained for the 100° C calcium hydroxide treated specimens. This value corresponds to an improvement in strength of ~2.4 times above the controls and 1.3 times greater than the 300° C D.I.-treated specimens. It should also be noted that the incorporation of spheres treated with the calcium hydroxide solution at the high temperature of 300° C results in a reduction in strength. Therefore, a temperature of up to ~200° C should be used. In this way, lightweight cementitious materials having a slurry density of $< 1.2\,g\,cc^{-1}$, a bulk density of $< 0.95\,g\,cc^{-1}$ after curing at 300° C, and a compressive strength of > 6.89 MPa at 24 h can be produced by incorporating the calcium hydroxide-treated microspheres.

It is worthwhile to assess the physico-chemical factors responsible for the significantly improved compressive strength of autoclaved lightweight cement specimens. Generally, good mechanical characteristics of composite materials can be attributed primarily to: (1) the degree of bond formation at the interface between the hydrated cement and the filler, (2) the phases formed and (3) the degree of hydration of the cement matrix. A microprobe evaluation of the interfacial region gives a better understanding of the mechanisms contributing to strong bonds. This information can be obtained from a combination of SEM morphological and EDX elemental detections at the failed lightweight cement surface after compressive strength testing, and can provide information on the nature of the interface and the cement reaction products formed near the sphere surfaces.

Fig. 9 shows SEM-EDX analysis of the untreated sphere-cement interface regions. The SEM images show that the failure propagates through the hydrated cement paste matrix and that many sphere particles which are covered with a layer of cement paste remain on the fractured surface. It is apparent from the failure mode and locus that the bond behaviour at the untreated sphere-cement hydration interface is very poor. An enlargement of a portion of the interfacial area identified as A in Fig. 9, shows that the hydrated cement paste in the boundary regions is porous. The presence of a large space in the contact zone also is indicated. This suggests that a porous cement hydrate layer, identified by EDX analysis as a $CaO-SiO_2-H_2O$ system, does not bond tightly with the sphere surfaces, thereby resulting in low compressive strength. The formation of these porous hydration products around the untreated sphere particles may be due to the presence of carbon contaminants diffused over the sphere surfaces.

Interest then was focused on the interfacial bond formation yielded by interactions between the calcium hydroxide-treated sphere surfaces and the hydrated cement paste matrix. Fig. 10 illustrates the typical SEM morphology and EDX analysis in the interfacial regions. Referring to Fig. 10I, a low resolution study of the fracture surface indicates a distribution of a large number of craters, probably caused by the sphere particles being pulled away from the cement paste matrix. The number of spheres remaining, which are covered with a layer of cement paste, is very low. From the EDX analysis, the hydration product in the cement paste layer overlaid on the treated sphere surface seems to represent the formation of a silica-rich calcium aluminate hydrate system.

Considerable attention also was given to the morphological and elemental features at the crater-cement paste matrix boundary regions. Figure 10II is a high magnification view of area B. The high-resolution micrograph of the crater wall identified as site No. 1 in Fig. 10II indicates a peculiar lining of spinal-shaped dendritic particles. This dendrite lining layer was identified from the high X-ray intensity of aluminium in the EDX spectrum as an aluminium-rich calcium silicate hydrate system. In contrast, the phase morphology and EDX analysis for site No. 2 suggested that parts of the block-like crystal assemblages formed in direct contact with the craters are identical with the silica-rich calcium aluminate hydrate compounds similar to the cement paste overlayer confirmed in Fig. 10I. The fact that two different phases are present within ~5 μm depths from the edge of the lining wall towards the hydrated cement matrix is interesting. The aluminium-rich wall seems to be related directly to the formation of intermediate layers produced by an interfacial interaction occurring between the cement paste and the epitaxial $CaO-Al_2O_3-SiO_2-H_2O$ layer overlaid on the calcium hydroxide-treated surface. These intermediate layers formed in the contact layer-to-cement paste interfacial transition zone may promote cross-linking and coupling functions which tightly connect the cement matrix with the sphere filler, thereby resulting in increased compressive strength.

From the standpoint of failure, it appears from the large number of craters in the fractured surfaces that loss of adhesion in the cement matrix/intermediate layer/contact layer/sphere filler bonding system occurs most frequently at the intermediate/contact layer interface. This may be due to the crystallization pressure caused by the growth of the aluminium-rich crystal product formed in the transition zones. The settlement of a well-crystallized intermediate layer would result in the separation of the cement matrix from the contact layer.

The magnitude in reactivity of the epitaxial contact layers depends on the temperature of the calcium hydroxide solution and the treatment time. The precipitation of this adherent layer on the sphere surface leads to its conversion into a well-crystallized intermediate layer as a result of an interfacial reaction with the cement paste in a hydrothermal environment.

As discussed earlier, the data given in Table I indicate that the compressive strength for 300° C calcium hydroxide sphere-filled cement specimens is lower than those for spheres treated with 100 and 200° C calcium hydroxide solutions. This reduction in strength was postulated to be due to an interfacial separation of the cement matrix from the contact layer, resulting from the production of a highly crystallized intermediate layer.

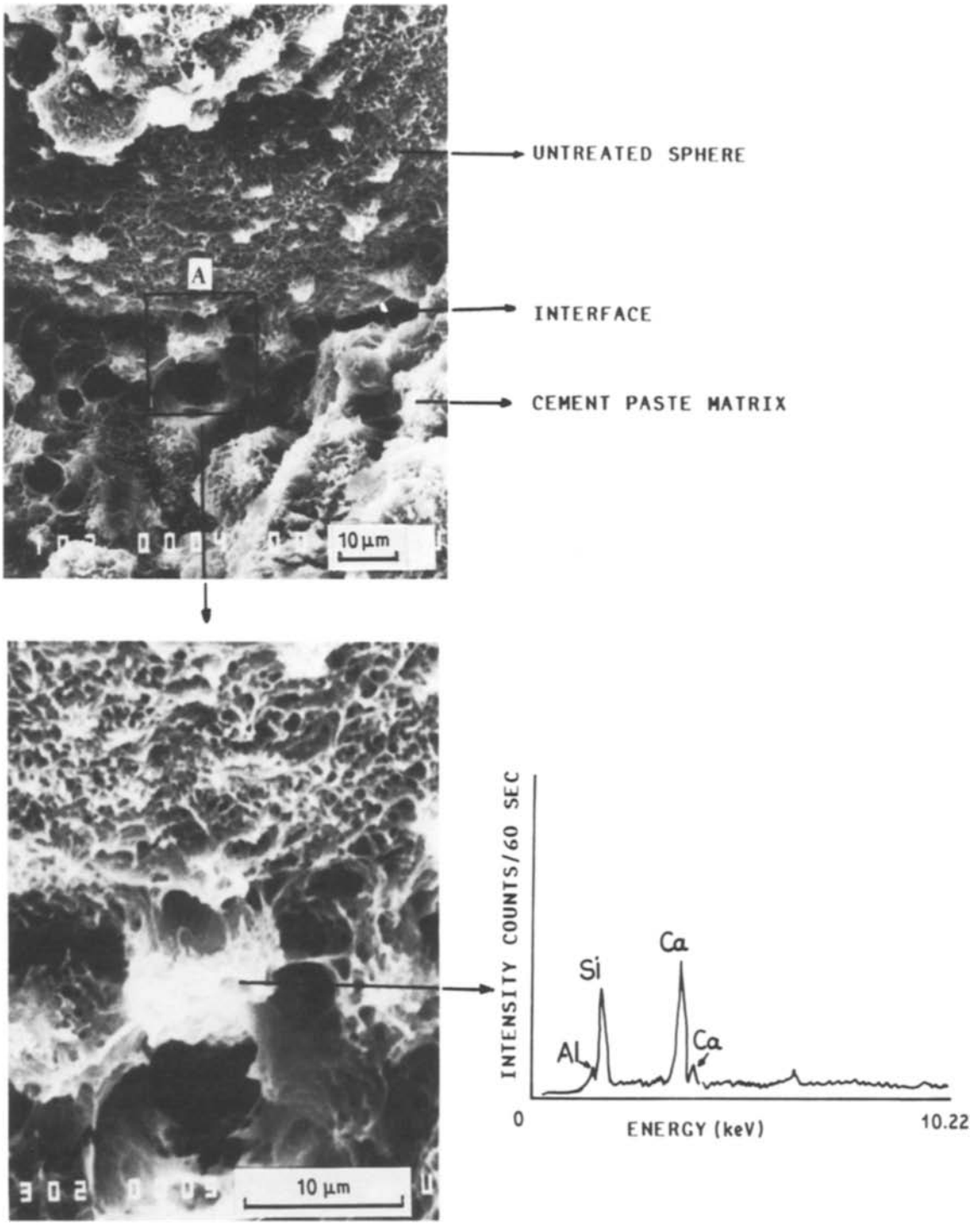

Figure 9 SEM micrographs and EDX analysis at contact zone between the untreated sphere and the hydrated cement for the fractured surfaces of 300° C-24 h autoclaved specimens.

To clarify the extent of interaction between the cement paste reactant and the contact layer, this interface was studied with the techniques described above; the results are shown in Fig. 11. Site No. 3 on the SEM micrograph shows that a well-crystallized dense intermediate layer is formed after 24 h exposure in the autoclave at 300° C. The thickness of this dense crystal layer which is representative of the rim-like structure, was roughly 4 μm. The EDX spectrum of the rim (also given in Fig. 11) indicates that a significant quantity of aluminium is present. This finding implies that the large amount of aluminium ion needed to form the thick aluminium-rich calcium silicate hydrate crystal layer has migrated to the cement paste reactant from the contact layer, which can be expressed as a chemically reactive layer. Site No. 4 located at a distance of $\sim 10\,\mu$m from the edge of rim was identified by EDX analysis to be a well-crystallized $CaO-SiO_2-H_2O$ matrix.

Preliminary EDX examinations of sites at distances of $\sim 6\,\mu$m from the rim edge revealed a distribution of elemental peak intensities similar to those detected from site No. 2 in Fig. 10II. Thus, the rim-cement matrix interface appears to consist primarily of three layers: (1) an $\sim 4\,\mu$m thick rim containing a high concentration of Al_2O_3 and low amounts of SiO_2 and

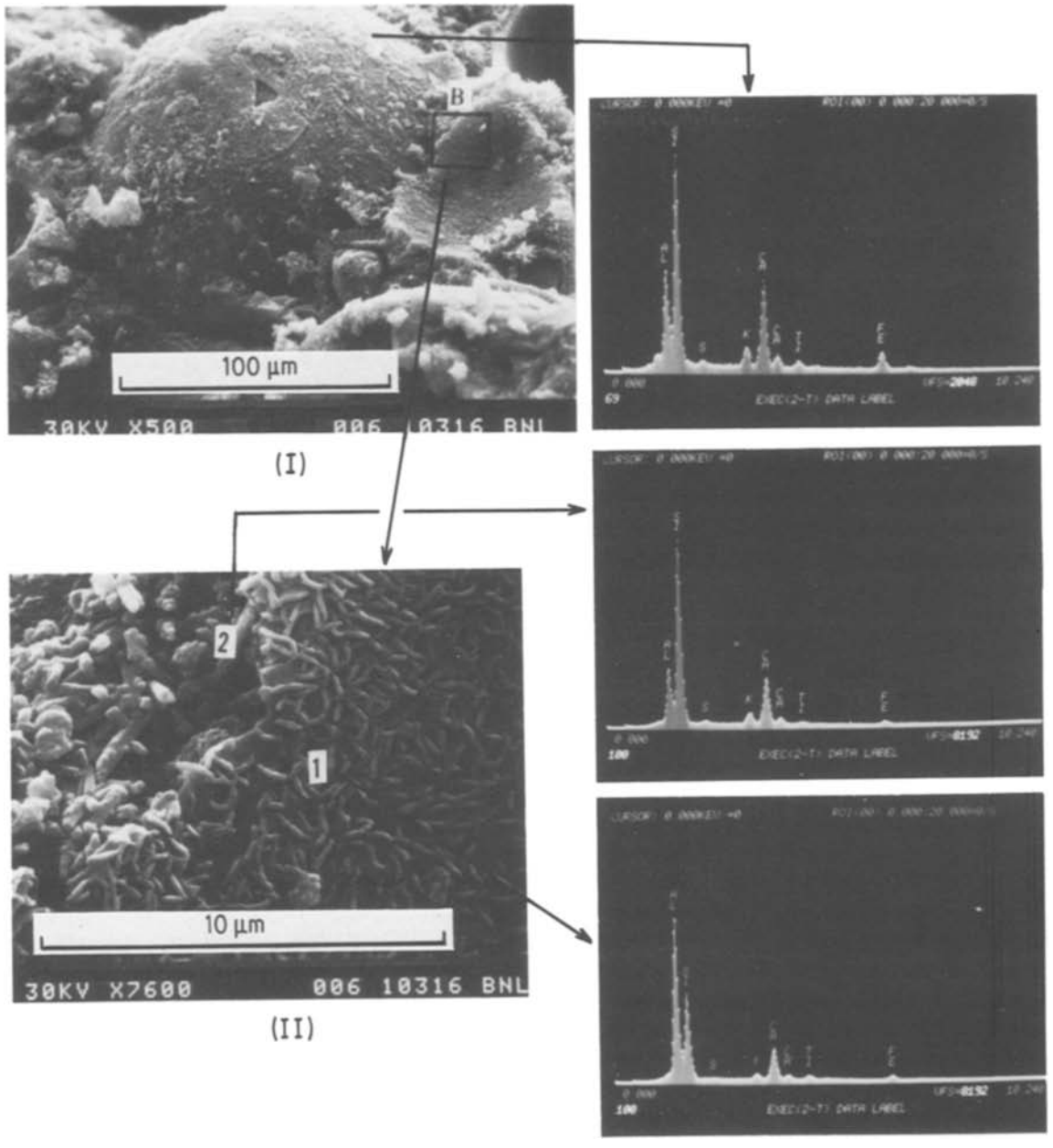

Figure 10 SEM images and EDX spectra on fracture surface of cement composites made with calcium hydroxide-treated spheres after exposure for 24 h in autoclave at 300° C.

CaO, (2) an interfacial layer ($\sim 3\,\mu$m thick) formed at the rim-cement matrix boundary which contains a high SiO_2 concentration and low amounts of Al_2O_3 and CaO, and (3) a highly hydrated cement matrix containing high SiO_2 and CaO and low Al_2O_3.

The improvement in compressive strength exhibited by the sphere-filled lightweight cements after autoclaving at 300° C is not only due to bonding at the cement matrix-sphere interface, but also relates to the phase and the extent of cement hydration in the bulk cement paste matrix. XRD analyses with Cu$K\alpha$ radiation gave information on the latter. XRD tracings in the diffraction range 0.342 to 0.288 nm were recorded for three different formulations, untreated spheres-cement paste, 200° C D.I.-treated spheres-cement paste, and 100° C calcium hydroxide-treated spheres-cement paste. The results are given in Fig. 12.

For the untreated sphere-cement systems, the XRD pattern indicates the presence of a large amount of unhydrated cement reactant and residual quartz (Fig. 12a). These are shown by the strong line at 0.334 nm for the quartz (Q) and the medium intensity line at 0.303 nm for the reactant (R). The weak intensities of the lines at 0.306 and 0.296 nm in this pattern reveal the formation of poorly crystallized tobermorite (T).

The inclusion of 200° C D.I.-treated spheres in the formulation resulted in the growth of a basal spacing at 0.306 nm and a reduction in peak intensity at 0.303 nm (Fig. 12b). This suggests that the moderately crystallized tobermorite, along with a lesser amount of reactants, are formed by incorporating the 200° C D.I.-treated spheres. Based upon these results, it is concluded that carbon contamination existing on the untreated sphere surfaces substantially retards or halts the progression of the hydration reactions, thereby resulting in lower strength cements. Tracing C for the calcium hydroxide treated sphere-cement systems exhibits better crystallinity of tobermorite than the other and also a moderate amount of reactants. The

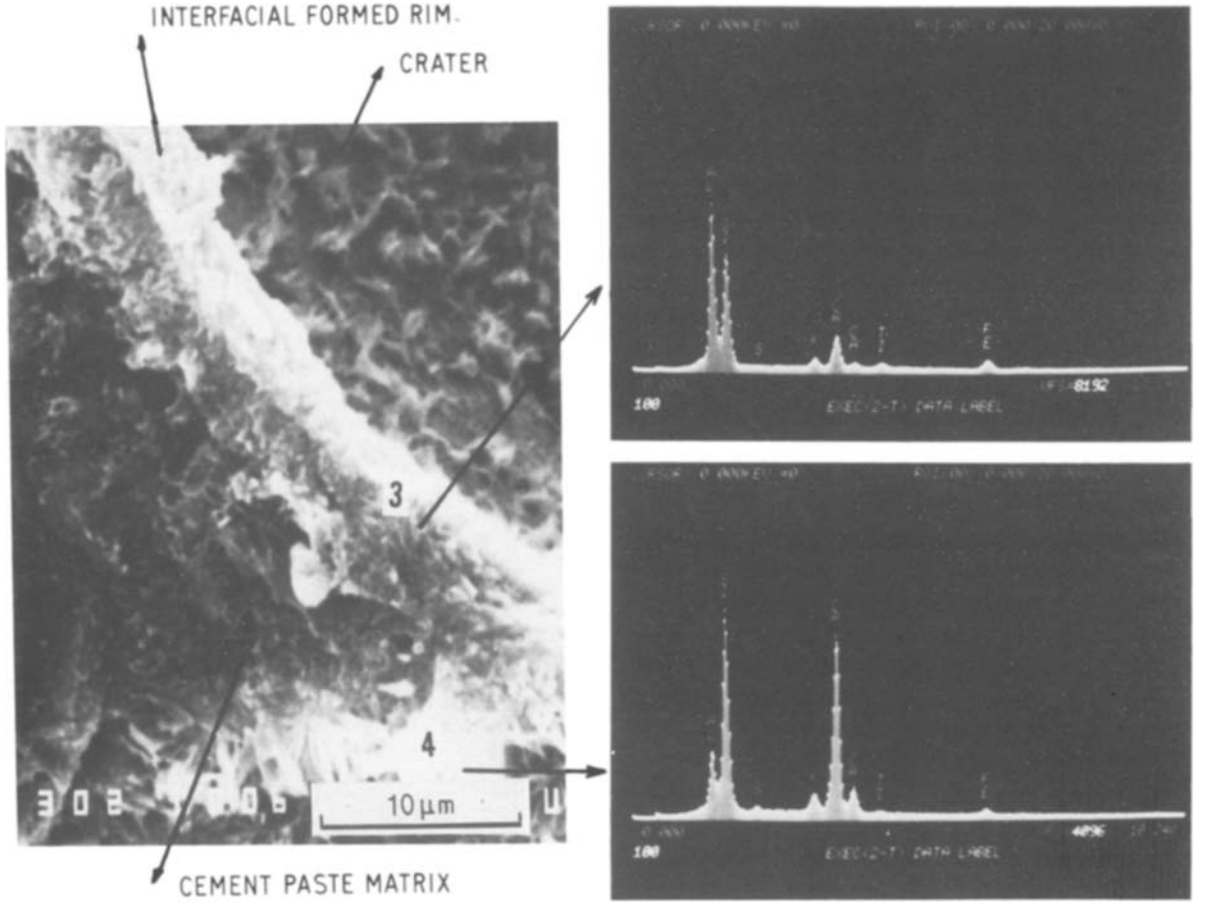

Figure 11 Morphological features and X-ray spectra at the interfacial region between intermediate layer and cement paste matrix.

strong basal spacing at 0.306 nm can be ascribed to the formation of well-crystallized tobermorite. This implies that the epitaxy formed on the calcium hydroxide-treated sphere surfaces results in a significant increase in the hydration rate of the cement paste matrix.

4. Conclusions

It was determined that in high temperature lightweight cementing materials containing pressure-resistance hollow microspheres, the presence of carbon contaminant on the "as-received" microsphere surfaces significantly suppressed the development of compressive strength upon curing in a 300° C hydrothermal environment. The typical microstructure of the contact zone formed at the cement matrix-to-untreated sphere interface was highly porous, thereby resulting in weak adhesion. A thin continuous overlayer consisting of the carbon contaminant, SiO_2 Al_2O_3, and hydrated aluminium oxides was demonstrated at the outermost surface sites of the untreated spheres. This overlay can be removed by treatment with D.I. water at a temperature of 200° C. Upon removal, an underlying crystal shell material was detected which exhibited a reticulated network structure of sillimanite containing γ-Fe_2O_3, FeO, and Fe_3O_4. The sillimanite surface had a strong affinity for bonding with the cement matrix, and was responsible for enhancement of the compressive strength of the lightweight cements.

In the characterization of sphere surfaces that were treated with a calcium hydroxide-saturated solution of

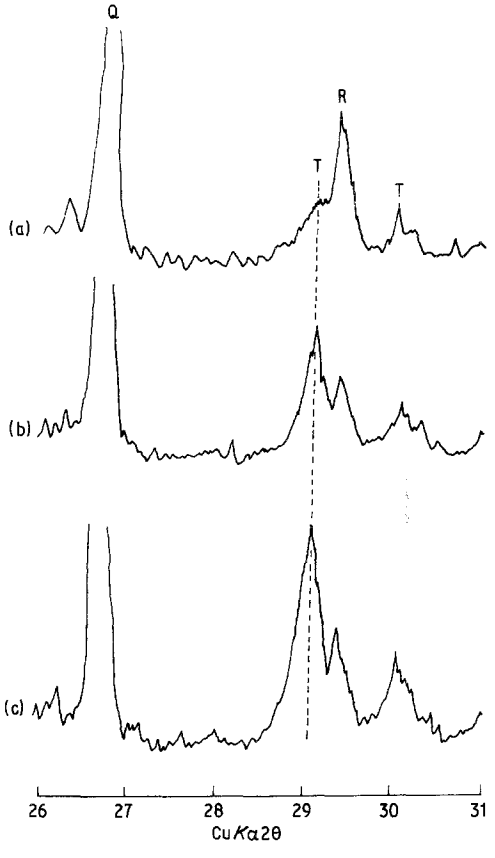

Figure 12 XRD tracings for (a) untreated sphere-cement, (b) 200° C D.I.-treated sphere cement and (c) 100° C calcium hydroxide-treated sphere cement systems autoclaved for 24 h at 300° C. Q:quartz, T: tobermorite, R: cement reactant.

up to 200° C, the epitaxial layers precipitated by the interaction between the hot solution and the overlayer played an important role in developing cement paste-to-sphere interfacial bonds and in enhancing the extent of hydration of the cement matrix. The major constituents of this epitaxy seem to be $CaO-Al_2O_3-SiO_2-H_2O$ and $CaO-SiO_2-H_2O$ systems. The interaction occurring at the epitaxy-to-cement paste interfaces under the hydrothermal environment at 300° C led to the formation of a highly dense intermediate rim structure, which was identified as an aluminium-rich calcium silicate hydrate compound. This $\sim 4\,\mu m$ thick intermediate layer contributes greatly to an increase in the magnitude of coupling and cross-linking functions connecting the spheres and the cement matrix. However, the highly crystallized intermediate layer results in failure of adhesion because of crystallization pressure at the epitaxy/intermediate layer interface.

The developed compressive strength for 300° C 24 h autoclaved specimens was not only dependent on the bonding characteristic at the matrix/sphere joints, but also related directly to the phase species and degree of hydration of the cement paste matrix. The morphological features of the cement matrix for the untreated sphere-filled cement systems indicate a porous body structure, consisting mainly of a large amount of reactant and a poorly crystallized tobermorite phase. This suggests that the presence of carbon contaminants act to retard the cement hydration processes. In contrast, the addition of the D.I.- and calcium hydroxide-treated spheres had significant effects on the formation of well-crystallized tobermorite along with the presence of a moderate amount of reactants.

Acknowledgements

The authors would like to thank H. C. Hua, State University of New York at Stony Brook, for providing the XPS data. This work was performed under the auspices of the U.S. Department of Energy, Washington, D.C. under Contract No. DE-AC02-76CH00016.

References

1. T. SUGAMA, L. E. KUKACKA and B. G. GALEN, in Proceedings of Annual Meeting of Geothermal Resources Council, Palm Springs, California, September, 1986.
2. M. MARTIN, Proceedings of the 3rd International Seminar of EC Geothermal Energy Research, Munich, Germany, November 1983, p. 447.
3. N. IWASAKI and Y. TOMIYANA, Review of the 30th General Meeting of the Cement Association, Japan, (1976) p. 213.
4. B. D. BARNES, S. DIAMOND and W. L. DOLCH, *Cem. Concr. Res.* **8** (1978) 233.
5. L. STRUBLE, J. SKALNY and S. MINDESS, *ibid.* **10** (1980) 277.
6. R. ZIMBELMANN, *ibid.* **15** (1985) 801.
7. Card 10-369, Joint Committee of Powder Diffraction Standards, (1984).

Received 8 January
and accepted 13 March 1987